Front. Mech. Eng. 2018, 13(1): 3–16
https://doi.org/10.1007/s11465-018-0475-0

RESEARCH ARTICLE

Dexin MA

Novel casting processes for single-crystal turbine blades of superalloys

Abstract This paper presents a brief review of the current casting techniques for single-crystal (SC) blades, as well as an analysis of the solidification process in complex turbine blades. A series of novel casting methods based on the Bridgman process were presented to illustrate the development in the production of SC blades from superalloys. The grain continuator and the heat conductor techniques were developed to remove geometry-related grain defects. In these techniques, the heat barrier that hinders lateral SC growth from the blade airfoil into the extremities of the platform is minimized. The parallel heating and cooling system was developed to achieve symmetric thermal conditions for SC solidification in blade clusters, thus considerably decreasing the negative shadow effect and its related defects in the current Bridgman process. The dipping and heaving technique, in which thin-shell molds are utilized, was developed to enable the establishment of a high temperature gradient for SC growth and the freckle-free solidification of superalloy castings. Moreover, by applying the targeted cooling and heating technique, a novel concept for the three-dimensional and precise control of SC growth, a proper thermal arrangement may be dynamically established for the microscopic control of SC growth in the critical areas of large industrial gas turbine blades.

Keywords superalloy, investment casting, Bridgman process, directional solidification, single crystal, turbine blade

1 Introduction

Turbine blades fabricated from Ni-based superalloys are widely used in aero-engines and industrial gas turbines (IGT). From a material property perspective, the limiting component of a gas turbine is the first-stage blade, which is under the highest gas-temperature stresses (Fig. 1). Ni-based superalloys are the preferred material for turbine blades given their high temperature strength, microstructural stability, and corrosion resistance. Improvements in casting methods and the chemical composition of alloys used for the production of rotor blades have directly increased rotor inlet temperature, subsequently increasing efficiency. Casting methods have been improved from conventional investment casting, which produces an equiaxed (EQ)-grain structure, to directional solidification (DS), which produces columnar-grain (CG) and single-crystal (SC) structures. Although polycrystalline Ni-based superalloys are inherently strong, their properties can be further improved through processing. In the case of rotor blades where the primary stress axis is along the length of the blade, aligning grains along the stress direction can improve creep rupture life, creep rupture ductility, and thermal fatigue resistance [1–3]. DS is used to produce oriented CG or SC structures to align or completely eliminate grain boundaries. Developments in chemical composition and advanced processing have enabled the fabrication of Ni-based superalloys with capabilities far beyond that imagined at the beginning of superalloy development. Advancements in alloy composition have resulted from modifying different casting techniques, as well as generational developments, and have subsequently improved the high-temperature capabilities of alloys. SC superalloys are currently used in increasing quantities in gas turbine engines (Fig. 1), although the use of castings in the columnar and EQ forms remains practical in many instances.

Turbine blades are typically produced in an investment casting process, which has also been called lost wax and precision casting. This method is especially suitable for casting components with complex and near-net shape geometry. Casting begins with the preparation of the wax pattern of the final component by injecting molten wax into

Received April 4, 2017; accepted July 3, 2017

Dexin MA (✉)
Wedge Central South Research Institute, Shenzhen 518045, China
E-mail: d.ma@d.ma.rwth-aachen.de

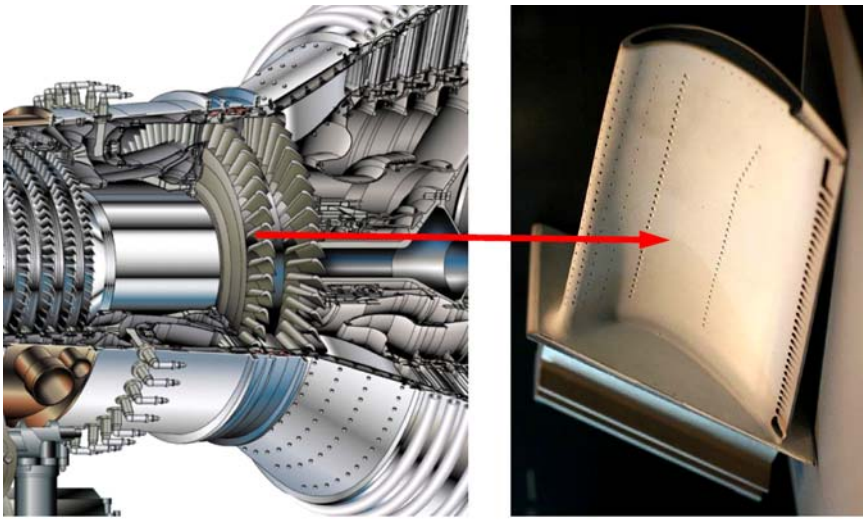

Fig. 1 (a) High-pressure turbine rotor assembled with (b) SC blades

a metallic die with a ceramic core, which is a replica of the required cooling passages in hollow blades. To produce SC blades, the wax patterns should be welded with grain selectors at their bottom. Large blade patterns for IGT are generally set up and processed individually. By contrast, small- and medium-sized patterns, such as those for the production of aero-engines, are usually assembled into cluster configurations, as shown in Fig. 2(a). This configuration produces several blades in a single casting cluster. The wax assembly is then repeatedly coated by dipping into ceramic slurries, followed by stuccoing with ceramic sands to build a ceramic shell mold around the wax pattern. The shell mold is de-waxed in a steam autoclave after the desired shell-wall thickness is attained (Fig. 2(b)). Prior to casting, the shell is fired in a heating furnace to develop the strength required to contain the molten metal.

Over the past years, rapid prototyping (RP) systems have been increasingly applied in wax-pattern manufacturing to reduce production time and costs [4–7]. However, owing to the "step effect" generated with the layer stacking and the surface roughness of the fabricated parts, RP technology remains limited to the production of single casting or small production units. The conventional investment casting process remains the only available option for the mass production of gas turbine blades with excellent surface finish. This process, however, suffers from long lead time and high tooling costs.

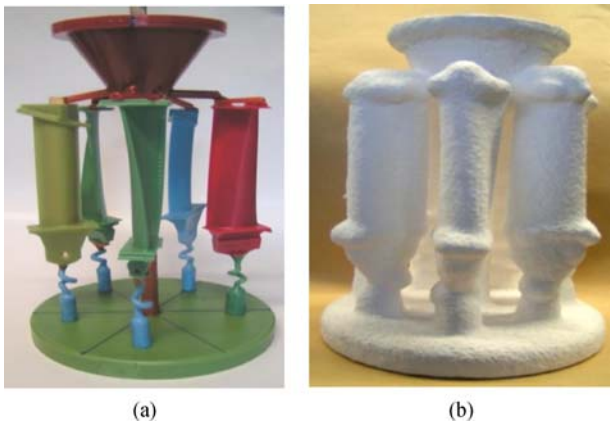

Fig. 2 (a) Circular-clustered wax assembly; (b) the corresponding shell mold manufactured for casting SC blades

The SC blades of superalloys are currently produced through the well-known Bridgman process [8–10]. A positive thermal gradient (G) sufficient for DS can be achieved by utilizing the concept of mold translation and a radiation baffle. A high G at the solidification front ensures sequential solidification along the axial direction and prevents EQ grains from initiating in constitutional undercooling zones within the melt. In addition, a fine microstructure with small dendrite spacing can be obtained with a high G, thus decreasing the time and cost of the heat treatment required to homogenize the highly alloyed materials. Therefore, processing technologies that allow for a high G in DS/SC process are necessary.

As shown in Fig. 3(a), the Bridgman furnace consists of an upper mold-heating chamber and a lower withdrawal chamber. These two chambers are separated by a radiation baffle. When a suitable vacuum is achieved, the mold is raised into the heating chamber, which is maintained at a temperature above the liquidus by a graphite heater. After pouring, the shell mold that contains the alloy melt is withdrawn at a programmed rate from the heating zone through the baffle into the cooling zone of the furnace. The withdrawal rate is typically set at a few millimeters per minute to allow the solid/liquid interface to progress gradually along the casting. This method has been

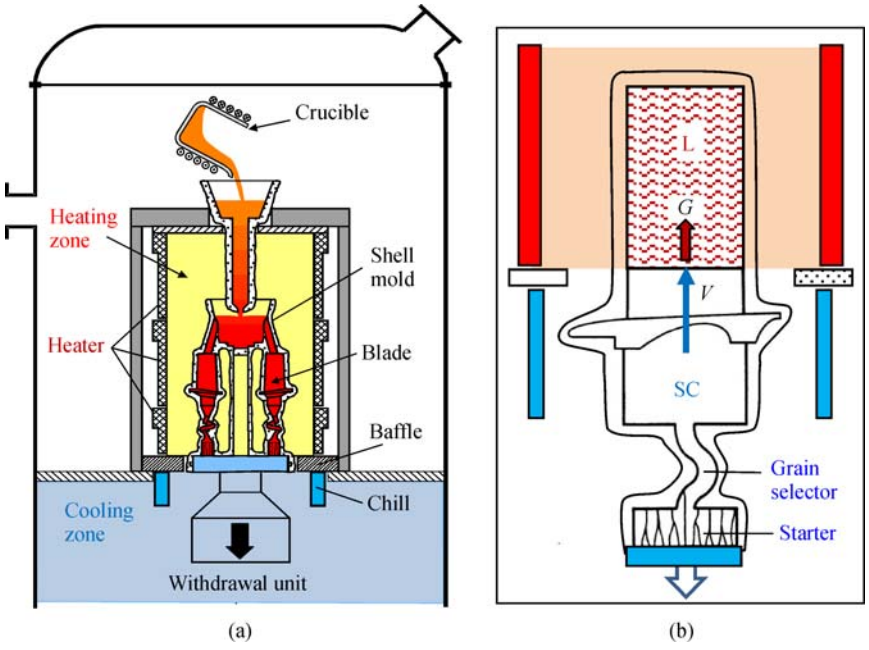

Fig. 3 (a) Schematic of a Bridgman furnace; (b) SC solidification with a grain selector

originally employed in the DS process to produce CGs, which are elongated in the direction of withdrawal such that transverse grain boundaries are absent. In a variant of this process, the grain boundaries are removed entirely. Grain boundaries are typically removed by adding a grain selector between the blade bottom and the starter top [9]. The grain selector is usually in the form of a pig-tail-shaped spiral (Fig. 3(b)). Given that the selector is not significantly larger in cross-section than the grain size, only a single grain enters the cavity of the casting, which then exists in monocrystalline form. Alternatively, a seed can be introduced to the base of the casting, provided the processing conditions are selected such that the seed is not entirely remelted and growth occurs with an orientation consistent with that of the seed. Thus, a directional solidified SC structure will then be formed from the bottom to the top of the blades.

Modified Bridgman techniques, such as the liquid metal cooling technique (LMC), were developed to meet the demand for a highly efficient DS/SC casting process with high G. A schematic of the LMC process is shown in Fig. 4 [11]. Unlike in the conventional Bridgman process, the mold is withdrawn from the heating zone to a liquid metal bath after pouring in LMC. In this process, a dynamic floating baffle is used to isolate the heating and cooling zones of the furnace, thus improving G. In addition, a liquid metal is used as a coolant to cool the mold. The heat extraction method is modified to optimize convection instead of radiation. This process has considerable potential to solve the problems associated with the industrial production of large IGT components [12–15]. The liquid metal used in the LMC process can be Al, Sn, Ga-In alloy, or Ga-In-Sn alloy. The G values achieved with the LMC process are typically double those achieved with the Bridgman process. However, during the LMC process,

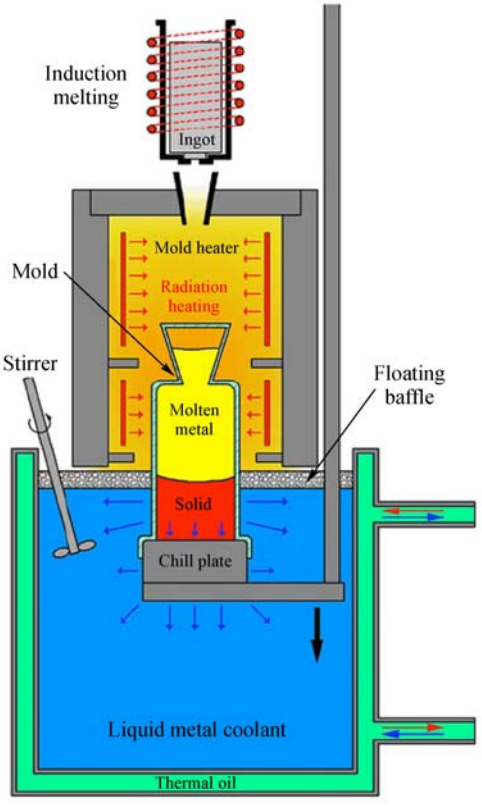

Fig. 4 Schematic of the LMC process [11]

the ceramic mold may crack because it suffers from considerable thermal impact when immersed in the liquid bath. Mold cracking allows the liquid metal to come in contact with superalloy components. In this case, the casting will be contaminated, and its performance will be degraded [16,17].

Although higher cooling rates and finer microstructures can be obtained through the LMC technique than those through the conventional Bridgman process, the LMC technique is still not widely employed in the industrial field given the high cost of equipment investment and complicated procedures, as well as the minimal improvement in casting quality. In fact, the increase in the magnitude of G during LMC is frequently accompanied by a change in the axiality of the temperature gradient and the curvature of the solidification front [13]. That is, heat is extracted so efficiently that G becomes non-axial for LMC casting. Lateral growth occurs during conventional Bridgman processing when the solidification front is lowered into the cooling zone of the furnace because of the high pulling velocities or drastic changes in geometry. Lateral growth considerably increases during LMC compared with during the conventional Bridgman process [13,18].

Figure 5 shows the gas cooling casting (GCC) process, which was developed by Konter et al. [18] at ALSTOM Power Technology for the manufacture of large SC components. The GCC process provides further improvements upon the conventional Bridgman process. Apart from radiation cooling, an inert gas is injected directly below the furnace baffle to cool the casting as it is withdrawn from the heating zone. According to Ref. [18], the achieved G in the front of liquid/solid interface in the GCC process is twice than that in the conventional Bridgman process. However, owing to the opening between the heating and cooling chamber, the cooling gas must inevitably blow upward into the heating chamber. This effect considerably decreases the furnace temperature and the temperature gradient in the alloy melt, thus negatively affecting the DS/SC process of the components in the shell mold. This unavoidable problem limits the wide industrial application of the GCC processes.

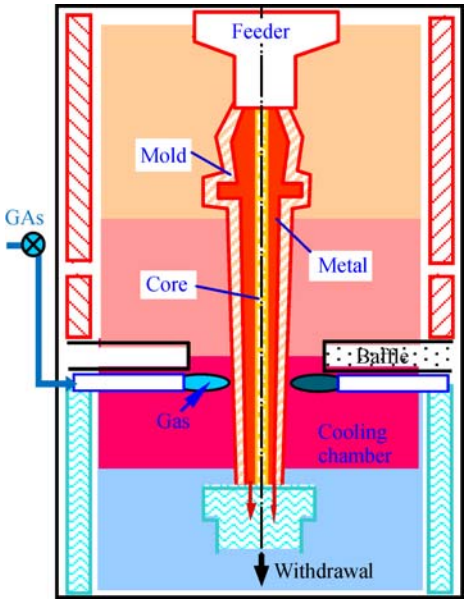

Fig. 5 Schematic of the GCC process [18]

In the LMC or GCC techniques, the entire casting is intensively cooled by a liquid metal bath or a cooling gas around its perimeter. The casting portions surrounded by thin shell-mold walls, such as the trailing edge of the airfoil and the extremities of platform, are more affected by the coolant than those surrounded by thick shell-mold walls, such as the junction between the airfoil and platform. As a result, inhomogeneous cooling in the casting becomes pronounced and is less favorable for stable and controllable SC growth. Over the past few decades, unremitting efforts have been exerted to develop alternative processes for industrial production. However, few significant modifications to the SC casting process have been reported.

2 Geometry-related grain defects in SC blades

Given their potentially detrimental effects on mechanical properties, structural defects are of primary importance in setting acceptance standards for SC castings during inspection. Stray grains (SGs) are the most serious structural defect in SC castings and cannot be tolerated because they introduce random crystal orientation and the high-angle grain boundaries. The properties of castings with this defect are lower than those of EQ castings because of the absence of boundary-strengthening elements.

SGs appear in several forms. When the vertical temperature gradient is insufficient to sustain directional growth, SC transitions to EQ grains, leading to the random nucleation of SGs ahead of the liquid-solid interface. In addition to the macroscopic thermal condition established in the Bridgman furnace, however, the geometry of the castings increasingly affects SG formation during SC process. SGs mainly occur at the extremities of the platform because of the abrupt transition of the cross-section and the rapid cooling of the local melt [19–27]. Figure 6(a) shows a schematic of the blade geometry and the formation location of a geometry-related SG. In the airfoil area, the SC growth of the primary grain is an undisturbed vertical DS process. However, crystal growth becomes lateral in the platform region. At the junction between the airfoil and the platform, a heat barrier zone (Fig. 6(b)) caused by the local poor cooling conditions appears. In this zone, the overheating of the alloy melt is prolonged and blocks SC growth from the airfoil into the undercooled platform. By contrast, the extremities of the

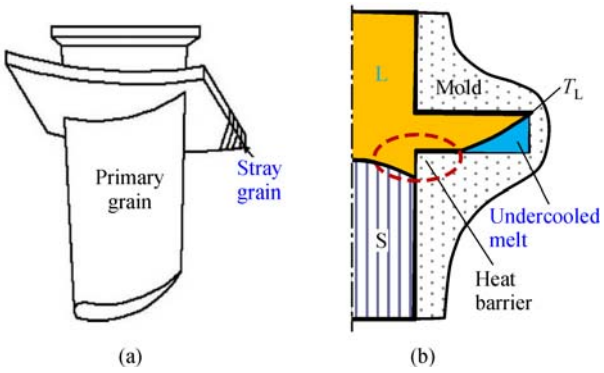

Fig. 6 (a) Schematic of the SG formation on the blade platform; (b) the corresponding heat barrier and melt undercooling region

platform cool rapidly. An isolated, thermally undercooled region of the melt forms as a result (Fig. 6(b)). When the local undercooling exceeds the undercoolability of the alloy, SGs nucleate before the arrival of the SC growth (primary grain) from the airfoil. The undercoolability of an alloy melt is its ability to be cooled to a temperature below the melting point without the onset of solidification. The undercoolability of an alloy can be evaluated by experimentally measuring critical nucleation undercooling in the shell mold [28].

Given that a superalloy often contains more than ten alloying elements, superalloys are among the most complex materials engineered by man. Despite having the same matrix element, Ni-based superalloys may have extremely different undercoolability values [28]. The chemical composition of the alloys, the process conditions, and the shell molds used influence undercoolability. Figure 7 shows the photographs of an etched turbine blade fabricated from a superalloy with a very low undercoolability value of only approximately 10 K. The figure also shows the formation of three SGs on the platform (Fig. 7(a)) and their further growth into the blade root (Fig. 7(b)). The used alloy is susceptible to SG formation because its low undercoolability value could be easily exceeded by local undercooling.

The undercoolability of an alloy is indicative of its ability to prevent the formation of geometry-related SGs.

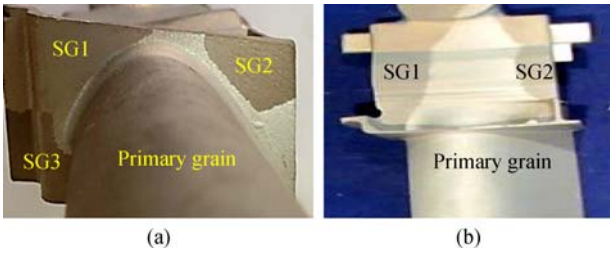

Fig. 7 (a) Turbine blade of a superalloy with low undercoolability, exhibiting SG formation on the platform; (b) SG growth into the blade root

For example, alloy CMSX-6 has an undercoolability of over 50 K [28]. At the platform extremities of the CMSX-6 blades, the melt can be intensively undercooled without exceeding its undercoolability. Under similar blade geometry and process conditions as those shown in Fig. 7, no SGs are observed in the CMSX-6 blades (Fig. 8(a)) because the nucleation of new grains is absent.

Lateral crystal growth can be observed in the transverse section of the platform (Fig. 8(b)). When the solidification front in the airfoil arrives at the nearest extremity at the trailing edge where a limited heat barrier exists, the primary SC dendrites can laterally grow from this position into the undercooled platform. The lateral SC growth in the platform first rapidly progresses along the cold edges into the highly undercooled extremities, turns inward toward the heat barrier zone with gradually decreasing velocity, and then finally meets the outward-going dendrites directly from the airfoil (Fig. 8(b)). However, in deeply undercooled extremities, as shown in Fig. 8(c), small dendrite arms are broken down from their parent trunks and become fragmented grains, as observed in Ref. [29]. From macroscopic observation (Figs. 8(a) and 8(b)), the matrix structure still resembles an SC because of the identical alignment of the dendrite trunks. However, microscopic investigation reveals fine misoriented grains between the dendrite trunks (Fig. 8(c)). The size of the misoriented grains is comparable with that of the secondary arm spacing of the dendrites. The existence of dendrite trunks indicates that initial nucleation can be excluded. The only mechanism for the formation of the misoriented grains appears to be the fragmentation of the secondary dendrite arms during local solidification. This structural defect is observed only in platform extremities with high undercooling capacity. Dendrite growth could still advance from the primary grain in the airfoil into the platform before initial grain nucleation occurs. However, rapid crystal growth into the highly undercooled melt initially results in a dendrite framework of thin primary and secondary arms. Given that the roots of the dendrite arms are thin and weak, partial remelting can occur during the subsequent coarsening process which begins with temperature recalescence upon the sudden release of latent heat. The broken arms become new fine grains with orientations different from their parent trunks due to drift and deflection. During this process, however, heterogeneous nucleation does not occur.

As found in a previous research [28], the superalloy CMSX-6 is highly undercoolable with a maximum undercooling temperature of approximately 50 K. However, instead of the dendrite structure, a fine EQ grain structure develops above the critical undercooling temperature of approximately 30 K. The interdendritic EQ grains observed in the present work is a transition structure that is slightly inferior to the critical undercooling. In this structure, the dendrite trunks are still in SC phase but the interdendritic grains are misoriented from the matrix

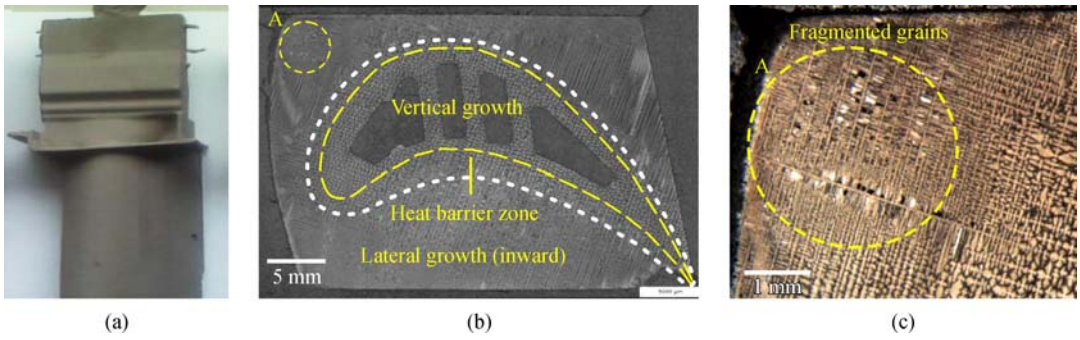

Fig. 8 (a) SC blade fabricated from alloy CMSX-6; (b) the transverse section of the platform showing the three-dimensional growth of SC dendrites; (c) fragmented grain defect in the deeply undercooled edge A

crystal and thus destroy local monocrystallity. Although SC can tortuously grow into the entire platform, the inhomogeneous microstructure degrades SC quality. Thus, thermal undercooling should be limited though the alloy provides a high undercooling capacity in ceramic molds.

As stated above, SC growth in a blade, especially in the platform region, is more complex than that in a solely vertical solidification process. Geometry-related defects, such as SGs (Fig. 7) and fragmented grains (Fig. 8(c)), cannot be removed by increasing G. Instead of intensifying the cooling of the entire component, special efforts should be considered to properly guide and control SC solidification along specific routes. In fact, the cooling rate of the blade extremities is already excessively high for SC solidification in conventional casting processes. Further increasing the cooling rate will aggravate defect formation. In the following sections, certain approaches for improving the production technique of SC blades by optimizing the Bridgman process will be presented. The use of these optimized processes can fully exploit the potential of SC components by producing defect-free as-cast structures.

3 Improvements in the casting technique

3.1 Grain continuator technique

To circumvent the heat barrier zone, a bypass (continuator) can be established for transferring the SC to the platform extremities [20], as shown in Fig. 9(a). For this purpose, during the assembly of the wax patterns, a thin wax bar of a few millimeters in diameter is attached between the adapter above the grain selector and the platform extremities susceptible to the formation of SGs. Solidification in the grain continuator (GC) advances faster than that in the blade airfoil because of the better cooling conditions in the GC. The solidification front will reach the platform before the alloy melt in the extremities becomes undercooled. The bypassed SC orientation can thus be transferred to the platform. However, during crystal growth in the GC, the orientation of the dendrite arms will twist differently from those in the blade section. As the inward growth of the bypassed dendrites meets the outward growth of the primary grain from the airfoil in the platform, the formation of subgrain boundaries becomes inevitable (Fig. 9(b)). After casting, the added GCs must be mechanically removed. Therefore, this technique cannot be employed for the production of casting parts, which require a net shape and cannot be machined.

3.2 Heat conductor technique

The heat conductor (HC) technique is another method used for suppressing SG formation at the platform extremities [29–32]. As shown in Fig. 6(b), a hot spot results from the poor local cooling condition at the junction between the airfoil and the platform. The heat barrier hinders epitaxial SC growth from the airfoil into the platform. By contrast, the outer extremity cools more rapidly than the hot spot because of the thinner mold wall in this region and the favorable view factor for heat radiation, leading to the rapid and deep undercooling of the local melt. In the HC technique, an HC is attached adjacent to the hot spots to minimize the heat barrier by improving the local heat

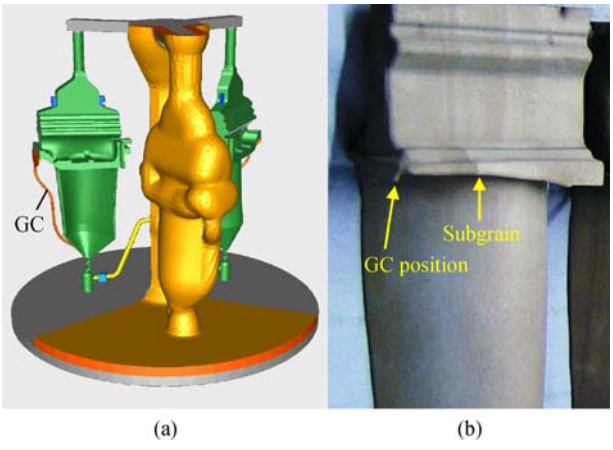

Fig. 9 (a) GC technique employed to avoid SG formation; (b) the subgrain boundaries between the bypassed grain and the primary grain from the airfoil

extraction conditions. Graphite is used as HC material because of its extremely high thermal conductivity compared with that of the ceramic mold. Moreover, graphite also has a high emission coefficient, which ensures effective heat radiation into the cold chamber of the Bridgman furnace.

Figure 10 shows the manufacturing procedure for the shell mold of a single blade. The ceramic shell molds are produced through a modified investment casting procedure. After finishing the first ceramic layer on the wax pattern (Fig. 10(a)) as in standard investment casting, the graphite HC is bonded at the locations selected using ceramic binder (Fig. 10(b)). The shell molds are processed to the final thickness through repeated dipping in ceramic slurries and sanding with fused alumina (Fig. 10(c)). In parallel, the exterior of the HC is cleaned with a toothbrush to remove ceramic accumulation.

In the corresponding experiments, the blades are cast in clusters, in which the blades are arranged in a circle around a central rod (Fig. 11). In each cluster, one half of the blades are bonded with HC (Fig. 11(b)) for comparison with the halves without HC (Fig. 11(a)).

Figures 11(a1) and 11(b1) show the simulated temperature development in the two shrouds without (left) and with (right) the application of HC, respectively. Both blades have similar external thermal conditions due to their symmetrical arrangement. The difference in temperature history can then be attributed solely to the application of HC. As shown in Fig. 11(a1), the isolated extremity of the original shroud remains thermally isolated for a long duration, thus becoming increasingly undercooled. This results in the formation of SG defects (Figs. 11(a2) and 11(a3)). By contrast, the bonded HC acts as a heat sink for the casting and effectively removes the hot spot at the junction between the airfoil and the shroud (Fig. 11(b1)). The undercooled extremity soon comes into contact with the primary crystal from the airfoil, from which an epitaxial crystal transition is introduced prior to the nucleation of SG, as experimentally confirmed (Figs. 11(b2) and 11(b3)).

In a series of casting experiments, the yield rate of acceptable blades improved from 37% to 100% compared with that of the conventional process [29]. Results indicated that the HC technique can effectively reduce geometrically-related SG formation. A better monocrystallinity can be achieved with the HC technique than that with the GC technique owing to the absence of subgrain boundaries (Fig. 9(b)). In addition, this technique can be employed for any section irrespective of machining limitations considering that no additional materials must be removed.

3.3 Parallel heating and cooling system

In a conventional Bridgman furnace, the heater and cooling chill have a cylindrical construction, as shown in Fig. 12. Correspondingly, a shell mold cluster for a group of parts is arranged in a circle around a central rod. During the Bridgman process, the heating and cooling condition is asymmetrical in the cast parts due to different radiation conditions. The temperature distribution and temperature gradient in castings have been investigated through 3D model simulations based on FEM (finite element methods) [33]. Results showed an asymmetric temperature distribution and a curved liquid-solid interface. Certain types of grain defects, such as SGs, formed differently on the two sides of the platform [34].

Based on the cylindrical construction of the Bridgman-type furnace (Fig. 12), the outside of the mold cluster can be immediately irradiated by the adjacent heater above the baffle. In the cooling zone below the baffle, this side can be effectively cooled by radiating heat to the adjacent chill ring. Therefore, an obviously high G for SC growth is provided on the outside of the mold cluster. However, the heat transfer condition is poor on the inward side of cluster that faces the central rod, inducing a shadow zone in the center of the cluster (Fig. 12).

As the mold cluster is withdrawn downward, the cylindrical shadow zone passes through the heating and cooling zones without the thermal isolation of the baffle

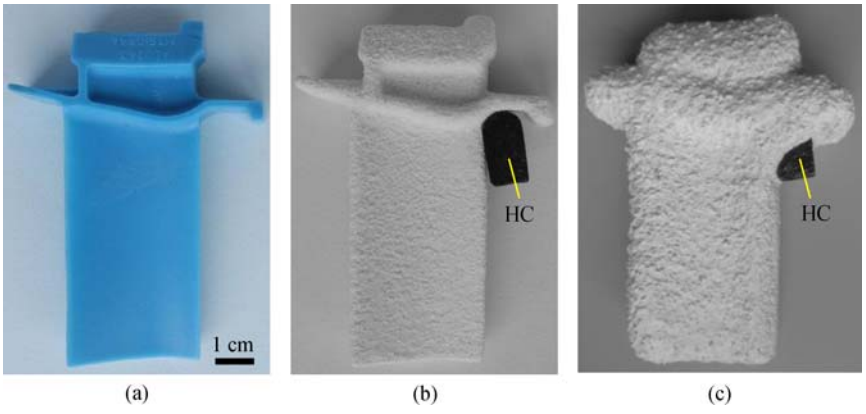

Fig. 10 Procedure of shell mold manufacture for HC insertion. (a) Wax model; (b) attachment of HC after the first layer; (c) finished shell mold for dewaxing [29]

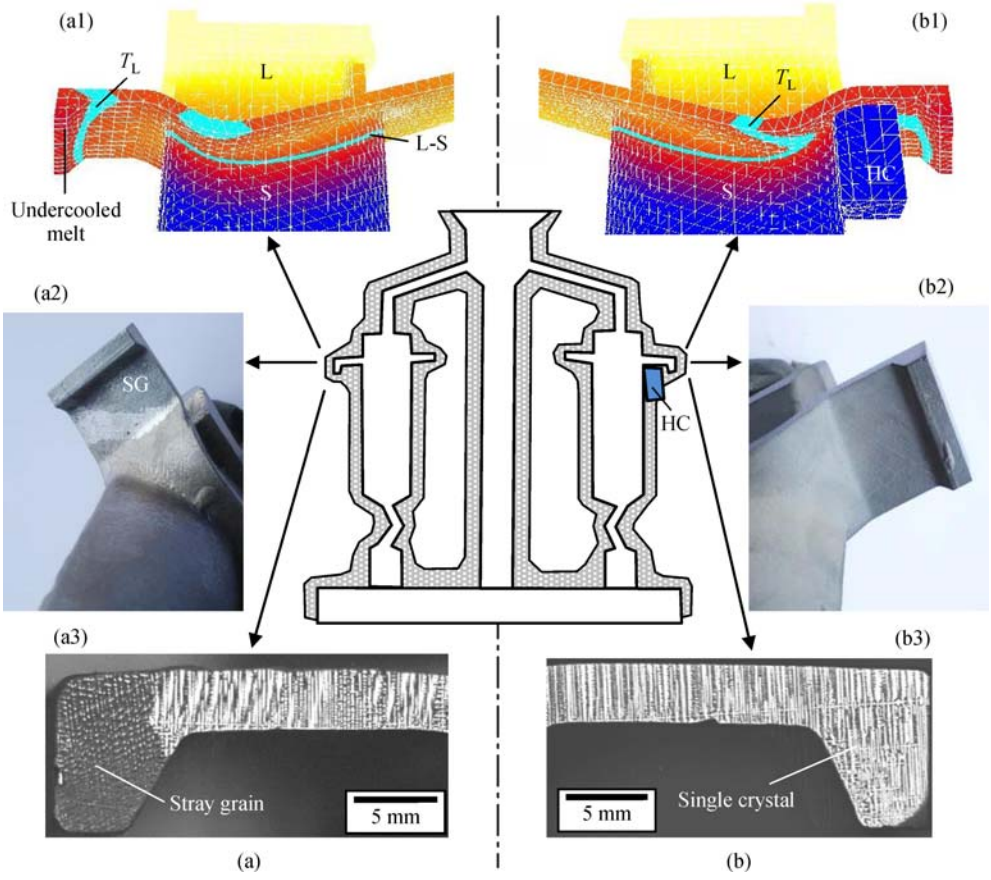

Fig. 11 Comparison of simulated temperature development (top), typical surface structures (middle) and microstructure in the blade platforms (bottom) between the castings without HC (left: (a1), (a2), (a3)) and those with HC (right: (b1), (b2), (b3)). (a) Without HC; (b) with HC

(Fig. 12(b)), similar to an opening at the bottom of furnace. This occurrence causes the loss of energy but also decreases G and extends the mushy zone. Therefore, the solidification condition on the inward side of the cluster becomes unfavorable for SC growth. Metallographic examination reveals a high susceptibility for SG formation [32,35] and freckling [36–39] in the shadow zone, whereas the heater side is less susceptible to these defects.

As stated above, the negative shadow effect is a typical disadvantage of the conventional Bridgman process. The cross-section area of the cylindrical shadow zone correspondingly increases with that of the heating chamber, particularly in large furnaces. The heating and cooling zone become less isolated due to the wider opening of the furnace base, leading to a more pronounced shadow effect. Therefore, a conventional Bridgman furnace cannot be built with an excessively large size because productivity cannot be simply increased as expected. Instead, the furnace size should be properly decreased to improve the quality of SC blades.

The parallel heating and cooling (PHC) system was developed to remove the negative shadow effect and achieve symmetric thermal conditions for the solidification of SC blades [30,39]. A schematic of the corresponding furnace construction with a double-row arrangement is shown in Fig. 13. Additional rows of heaters and cooling chills can be constructed in parallel to increase the casting productivity without any loss of SC quality due to the absence of the shadow zone that appears in the conventional Bridgman process.

In comparison with the conventional Bridgman furnace, the new furnace features a linear heater and cooling component. Correspondingly, the casting parts are aligned on a rectangular chill plate and can be symmetrically heated by the linear heater from both sides. After casting, the parts will be drawn downward into the cooling area and symmetrically cooled. The symmetric heating and cooling provides uniform thermal conditions with the benefit of optimizing microstructures and avoiding solidification defects. The heating and cooling zones are highly isolated due to the disappearance of the cylindrical shadow zone (Fig. 12), thus increasing G for SC solidification.

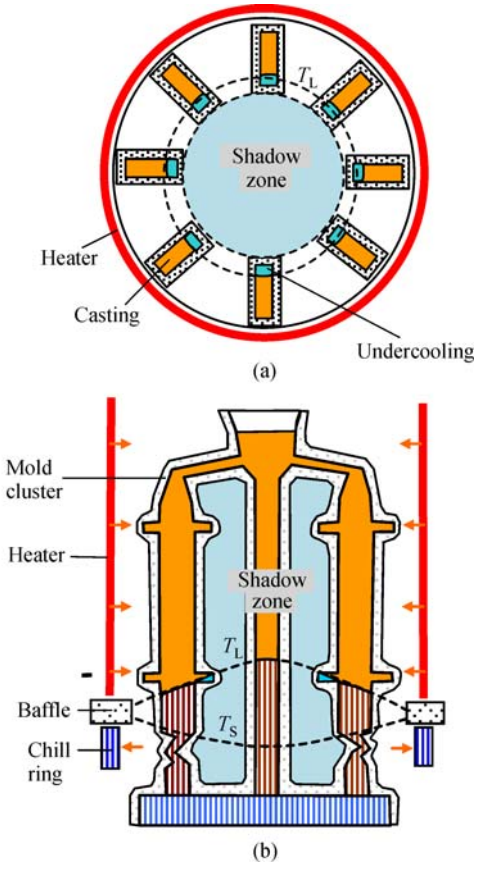

Fig. 12 Sketch of the cylindrical Bridgman furnace currently used for manufacturing SC blade clusters. (a) Transverse section; (b) longitudinal section

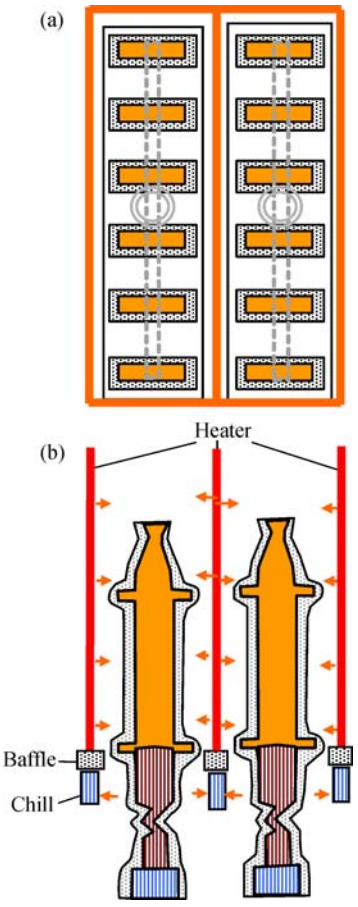

Fig. 13 Sketch of the PHC system. (a) Transverse section; (b) longitudinal section

Preliminary experiments with the PHC system have been performed in a pilot furnace with a single row arrangement. The casting cluster was linearly arranged so that both sides of a shell mold can be symmetrically heated in the heating zone and cooled in the cooling zone. For the casting experiments, the superalloy IN939 was selected owing to its strong tendency to form SGs [28]. The alloy melt was poured into the preheated shell mold mounted on the chill plate and then withdrawn from the hot zone into the cold zone through the baffle at a velocity of 3.0 mm/min. Corresponding experiments were conducted in a conventional furnace for comparison.

As expected, minimizing or eliminating the asymmetric thermal condition effectively suppressed SG formation. Few SGs were found in the specimens fabricated through the PHC system. Both sides of the specimens showed a minimal tendency for SG formation because of the improved symmetry of the thermal conditions. The SG ratio of the specimens significantly decreased from 49% to 6% compared with those of the specimens fabricated through the conventional Bridgman process [39]. These results confirmed the feasibility of the PHC system for improving the quality of SC components.

3.4 Dipping and heaving technology

A reasonably high temperature gradient for SC solidification is difficult to maintain with in the conventional Bridgman process because of the following reasons: (1) Ineffective radiative heat exchange, (2) unclosed baffle isolation between heating and cooling zones, and (3) high thermal resistance of the thick ceramic molds. Dipping and heaving (D&H) technology, also previously called thin shell casting [40] or downward directional solidification process [41], was developed [30,39] to mitigate these limitations. At the beginning of the D&H process, as shown in Fig. 14(a), a superalloy melt is overheated to a stable temperature in a crucible and covered with hollow ceramic beads, which function as a dynamic baffle. The ceramic mold, which has a selector (or an SC seed) connected to a chill at the top end, is dipped into the alloy melt through the dynamic baffle. To prevent the baffle beads from entering the mold, the bottom end of the mold is sealed by a stopper made from the same alloy. When the stopper has melted, the alloy melt flows into the mold and comes into contact with the chill-plate, leading to the nucleation of randomly oriented grains on the chill-

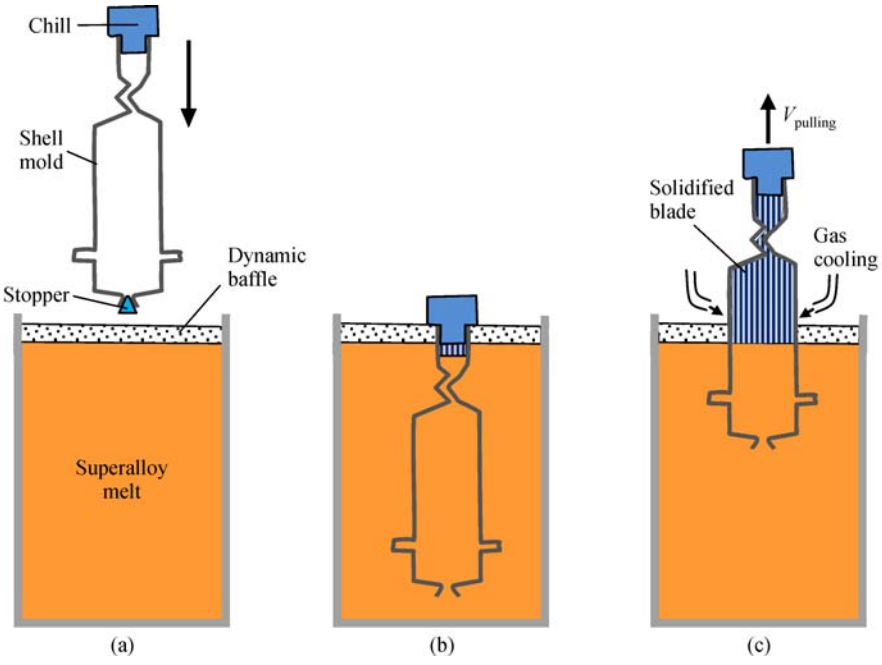

Fig. 14 Illustration of the D&H process. (a) Dipping the shell mold into the melt bath; (b) mold filling; (c) pulling up the mold to initiate downward solidification

plate and the competitive growth of columnar grains (Fig. 14(b)). When a relatively stable thermal condition is reached, the mold is pulled up from the melt bath at a specified withdrawal rate. SC growth will then occur through the grain selector during the downward solidification process of the blade (Fig. 14(c)). The shell mold can be additionally cooled by blowing inert gas as it is pulled up to provide greater heat extraction and enable faster withdrawal rates.

In the D&H process, owing to the balanced hydrostatic pressure exerted by the melt between the inside and outside of the mold, the wall thickness of the molds can be reduced to only approximately 1 mm, which is merely used to retain the casting's shape, as shown in Fig. 15.

D&H technology has been employed to produce SC superalloy blades under protective argon gas [41,42]. A D&H experiment is illustrated in Fig. 16(a). In this experiment, a thin-shell mold is used to manufacture an SC superalloy blade. Figure 16(b) shows an SC blade fabricated from superalloy CMSX-4 through D&H and a seeding technique, exhibiting a refined dendrite structure (Fig. 16(c)).

The thermal gradient G during solidification in the D&H process was measured as approximately seven times higher than in the conventional Bridgman process. A refined microstructure was correspondingly obtained. The structural parameters, such as the primary dendrite spacing, λ_1, the average size of the γ/γ' eutectic pools and the γ' precipitates, and the volume fraction of the micropores, significantly decreased, as shown in Fig. 17 and listed in Table 1. Given the refined structural scale of the material, short diffusion distances are provided to homogenize the material, subsequently decreasing the solution treatment times or enabling full solutioning during heat treatment for highly alloyed materials. In addition, the γ' precipitates produced were more finely and homogeneously distributed and were thus more beneficial than those obtained through the current Bridgman process.

The D&H technique has numerous advantages. Given

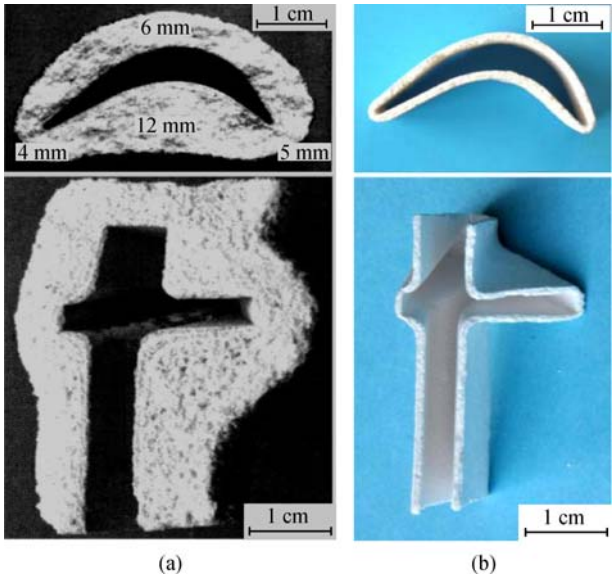

Fig. 15 (a) Wall thickness of the shell molds used for the production of turbine blades through the conventional Bridgman process; (b) through the D&H process

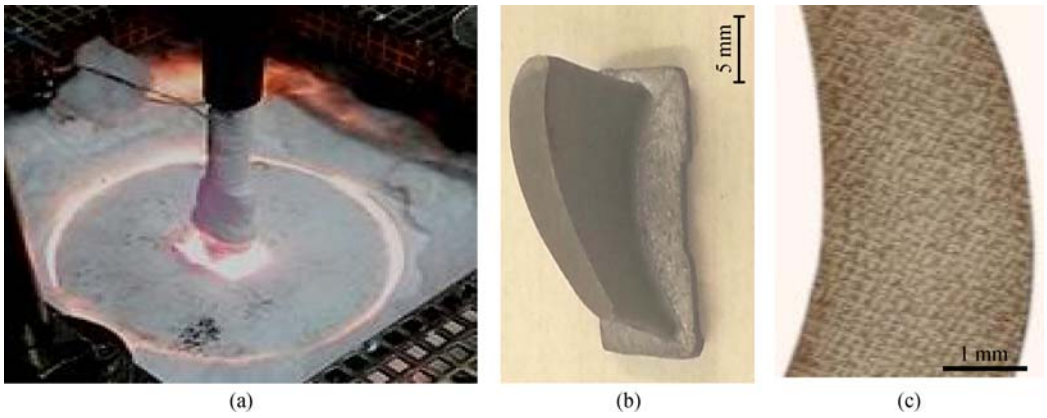

Fig. 16 (a) D&H experiment with a thin-shell mold to manufacture SC blade of superalloy CMSX-4; (b) as-cast blade; (c) transverse section

the use of extremely thin shell molds and the application of gas cooling, heat can be more efficiently extracted from the solidifying component in the D&H technique than in the conventional and modified Bridgman techniques. The heating and cooling zones can be well isolated using a dynamic baffle, thus increasing G at the solidification front. In the future, a large vacuum furnace for the D&H process should be built to enable the production of large IGT blades and aero-turbine blades in clusters for high productivity. Furthermore, a molten slag should be used as a floating baffle material to improve the isolation of the melt bath and facilitate its cleaning during the process, similar to that in the electroslag-remelting process.

Another important advantage of the D&H technique is the complete avoidance of freckle formation. Freckles, or channel segregates, are thin chains of EQ grains associated with localized heterogeneities in chemical composition. SC castings for both aeroengine and IGT applications can exhibit freckling. During the DS processing of superalloy components, light elements, such as Al and Ti, segregate into interdendritic regions, whereas heavy elements, such as W, Re, and Co, partition to the dendrite core [42–48]. As solidification proceeds, the alloy melt in the interdendritic regions at the bottom of the mushy zone becomes lighter. In the conventional process, the dendrites grow upward, leading to an inverse density distribution. The top-heavy melt in the mushy zone can result in thermosolutal convection, which destroys the dendrites and thus leads

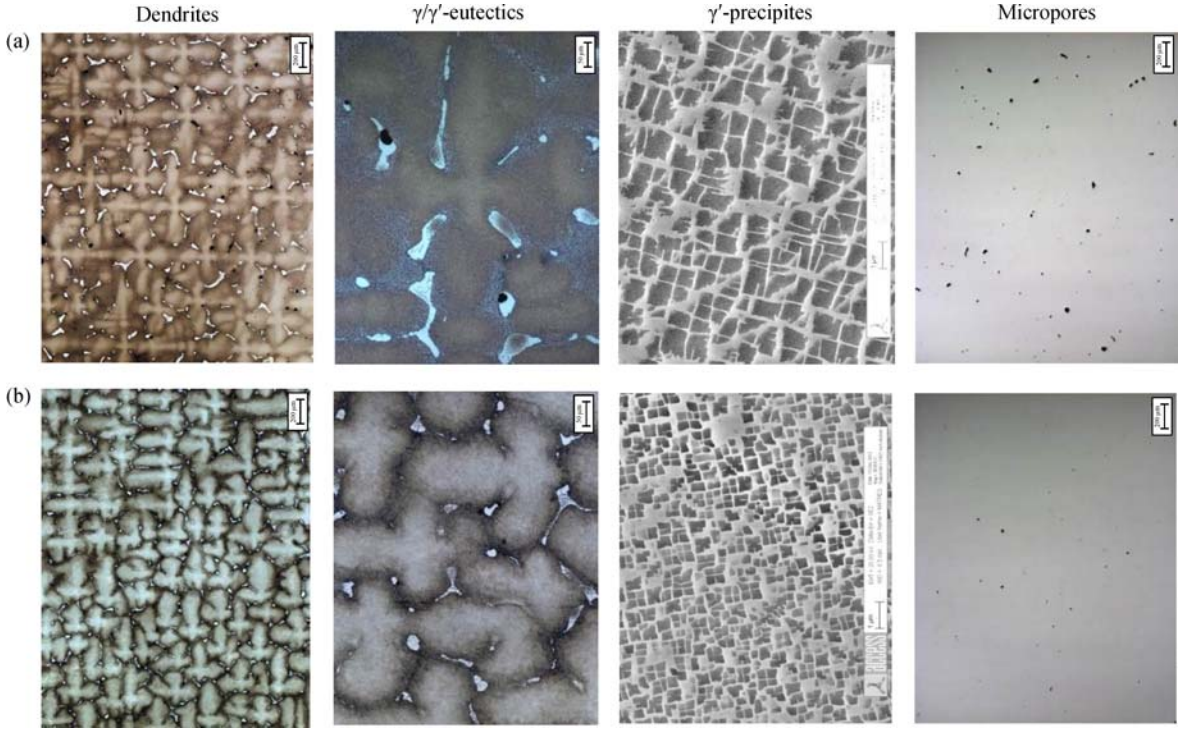

Fig. 17 Microstructure of CMSX-4 blades produced through the (a) Bridgman and (b) D&H processes

Table 1 Comparison of the process and structural parameters of the Bridgman and D&H processes

Process	G/(K·mm^{-1})	λ_1/μm	γ/γ'/μm^2	γ'/μm	Porosity/vol. %
Bridgman	2.2	445.6	1544.2	0.65	0.13
D&H	14.2	299.3	346.9	0.30	0.02

to the formation of freckle defects. The probability of freckling is strongly dependent on the composition of the alloy being cast. For example, third- or fourth-generation alloys rich in heavy elements, such as Re, are particularly prone to this effect. In the D&H process, the interdendritic melt becomes top-light due to the downward direction of solidification. Thus, the mushy zone is relatively stable, and the thermosolutal convection and the related freckle defects are essentially eliminated [49,50].

3.5 Precise control of SC growth through targeted cooling and heating

As stated above, D&H Technology generally provides excellent thermal conditions for SC solidification due to effective heat transfer. This technology can be further improved through combination with targeted cooling and heating (TCH) technology, which enables the establishment of a proper lateral thermal arrangement [30,39]. As shown in Fig. 18, gas cooling in the modified D&H process is not applied ubiquitously but is only aimed at the heat barrier zones (Position *B* in Fig. 18(a)) where lateral SC growth is hindered. Laser heating is applied at the platform extremities (Position *A* in Fig. 18(a)) where the alloy melt cools rapidly. The application of laser heating prevents undercooling in these regions and the subsequent formation of SGs. Furthermore, the dynamic control of SC growth can be achieved by simultaneously moving the TCH along a specified route from the airfoil into the extremities of the platform. Based on experimental data and numerical simulation, the intensity of cooling and heating will be controlled as a function of time and place to guide three-dimensional SC growth along an optimal route and sequence. The risk of undercooling and the related grain defects of the alloy melt can be completely removed due to the establishment of a positive thermal gradient ahead of the local solidification front. Though the extremities, such as at the Extremity *A* in Fig. 18(a), have an overhanging geometry, the local SC growth can still be precisely guided.

The TCH method can also be applied to the airfoil region of the blades (Fig. 18(b)). The trailing and leading edges (*C* and *D* in Fig. 18(b)) that cool too rapidly should be additionally heated using lasers. However, the thickest area of the airfoil, especially on the concave side (*E* in Fig. 18(b)), should be additionally cooled with gas injection to decrease the concavity of the local solidification front and to ensure a stable and homogeneous SC growth with high quality.

SC growth can be precisely guided along judicious routes to every edge of the blade by optimally employing the TCH technique. Due to the thin walls of the shell mold in the D&H process, the effect of the additional cooling and heating is more efficient and precise than that in the conventional Bridgman process. As a result, the microscopic and dynamic control of the local SC growth in three

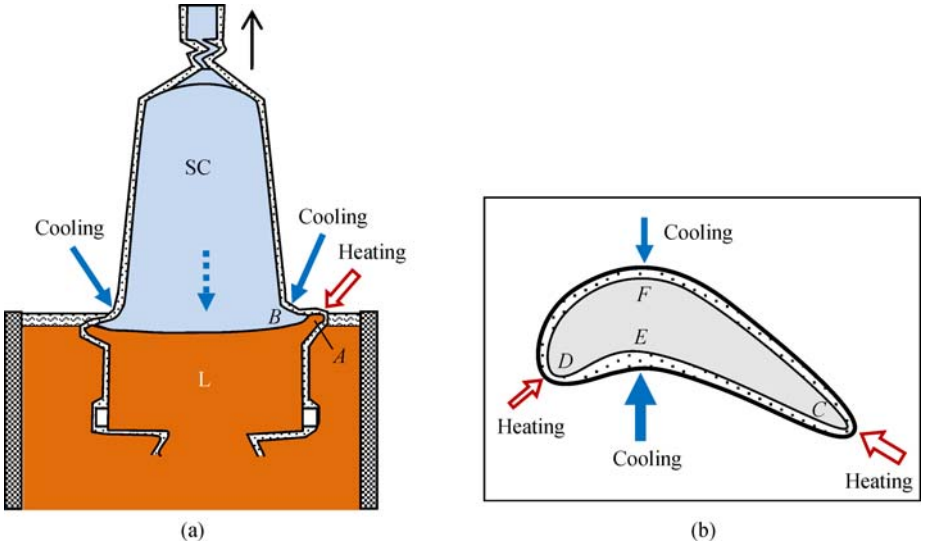

Fig. 18 Schematic of TCH in the longitudinal (a) and cross section (b) of a large turbine blade, to precisely control the local SC solidification in the platform and airfoil area respectively.

dimensions can be achieved in addition to the significant improvement in macroscopic cooling condition. Instead of injecting inert gas to strengthen the effectiveness of the process, dripping liquid Ar or He can be performed to achieve targeted cooling in this process.

4 Summary

This paper presents a brief review of the current casting techniques for SC blades, as well as an analysis of the solidification process in complex turbine blades. To remove geometry-related grain defects, the GC and HC techniques were developed to circumvent or minimize the heat barrier at the junction between the airfoil and the platform. Blades fabricated through the HC technique exhibit excellent monocrystallinity owing to the absence of subgrain boundaries. The PHC system has been employed to achieve symmetric thermal conditions for the solidification of SC blades. In this system, both sides of a shell mold can be symmetrically heated in the heating zone and cooled in the cooling zone. The negative shadow effect in the current Bridgman process and its related defects are thereby significantly reduced. The major problems with the Bridgman process, such as ineffective radiative heat exchange and high thermal resistance in the thick ceramic molds, can be effectively resolved through the D&H technique and the use of thin-shell molds. A fine microstructure can be obtained due to the establishment of a high G at the solidification front. A new concept for three-dimensional and precise control of SC growth was proposed on the basis of the analysis of the solidification process in complex turbine blades. The TCH technique was developed on the basis of this concept to establish a proper thermal arrangement for the microscopic control of SC growth in the critical regions of large IGT blades. The dynamic control of SC growth can be achieved by simultaneously moving the TCH along a specified route.

Acknowledgements This work was funded by the Science and Technology Innovation Commission of Shenzhen Municipality (Grant No. JSGG20141016141652366) and the Economic, Trade and Information Commission of Shenzhen Municipality (Grant No. 2016-122), the Program for Guangdong Introducing Innovative and Enterpreneurial Teams.

References

1. Versnyder F L, Shank M E. The development of columnar grain and single crystal high temperature materials through directional solidification. Materials Science and Engineering, 1970, 6(4): 213–247
2. Pratt D C. Industrial casting of superalloys. Materials Science and Technology, 1986, 2(5): 426–435
3. Quested P N, Osgerby S. Mechanical properties of conventionally cast, directionally solidified and single-crystal superalloys. Materials Science and Technology, 1986, 2(5): 461–475
4. Gebhardt A. Rapid Prototyping. Munich: Carl Hanser Verlag, 2006
5. Feriera J C, Santos E, Madureira H, et al. Integration of VP/RP/RT/RE/RM for rapid product and process development. Rapid Prototyping Journal, 2006, 12(1): 18–28
6. Budzik G, Markowski T, Sobolak M. Hybrid foundry patterns of bevel gears. Archives of Foundry Engineering, 2007, 7(1): 131–134
7. Pattnaik S, Jha P K, Karunakar D B. A review of rapid prototyping integrated investment casting processes. Proceedings of the Institution of Mechanical Engineers, Part L: Journal of Materials Design and Applications, 2014, 228(4): 249–277
8. Bridgman P W. US Patent, 1793672, 1931-02-24
9. Erickson J S, Owczarski W A, Curran P W. Process speeds up directional solidification. Metal Progress, 1971, 99: 58–60
10. Pratt D C. Industrial casting of superalloys. Materials Science and Technology, 1986, 2(5): 426–435
11. Elliott A J, Pollock T M, Tin S, et al. Directional solidification of large superalloy castings with radiation and liquid-metal cooling: A comparative assessment. Metallurgical and Materials Transactions A: Physical Metallurgy and Materials Science, 2004, 35(10): 3221–3231
12. Tschinkel J G, Giamei A F, Kearn B H. US Patent, 3763926, 1973-10-09
13. Giamei A F, Tschinkel J G. Liquid metal cooling: A new solidification technique. Metallurgical Transactions and Materials Transactions A: Physical Metallurgy and Materials Science, 1976, 7(9): 1427–1434
14. Elliott A J. Directional solidification of large cross-section Ni-base superalloy castings via liquid-metal cooling. Dissertation for the Doctoral Degree. Ann Arbor: The University of Michigan, 2005
15. Liu L, Huang T, Qu M, et al. High thermal gradient directional solidification and its application in the processing of nickel-based superalloys. Journal of Materials Processing Technology, 2010, 210(1): 159–165
16. Zhang J, Luo L. Directional solidification assisted by liquid metal cooling. Journal of Materials Science and Technology, 2007, 23: 289–300
17. Lohmüller A, Eßer W, Großmann J, et al. Improved quality and economics of investment castings by liquid metal cooling—The selection of cooling media. In: Proceedings of International Symposium on Superalloys. 2000, 181–188
18. Konter M, Kats E, Hofmann N. A novel casting process for single crystal gas turbine components. In: Proceedings of International Symposium on Superalloys. 2000, 189–200
19. Wagner A, Shollock B A, McLean M. Grain structure development in directional solidification of nickel-base superalloys. Materials Science and Engineering A, 2004, 374(1–2): 270–279
20. Meyer ter Vehn M, Dedecke D, Paul U, et al. Undercooling related casting defects in SC turbine blades. In: Proceedings of International Symposium on Superalloys. 1996, 471–479
21. Zhou Y. Formation of stray grains during directional solidification

of a nickel-based superalloy. Scripta Materialia, 2011, 65(4): 281–284

22. Tschinkel J G, Giamei A F, Kearn B H. US Patent, 3763926, 1973-10-09
23. Yang X L, Dong H B, Wang W, et al. Microscale simulation of stray grain formation in investment cast turbine blades. Materials Science and Engineering: A, 2004, 386(1–2): 129–139
24. Xuan W, Ren Z, Liu H, et al. Formation of stray grains in directionally solidified Ni-based superalloys with cross-section change regions. Materials Science Forum, 2013, 747–748: 535–539
25. Xuan W, Ren Z, Li C, et al. Formation of stray grain in cross section area for Ni-based superalloy during directional solidification. IOP Conference Series: Materials Science and Engineering, 2011, 27: 012035
26. Zhang J, Huang T, Liu L, et al. Advances in solidification characteristics and typical casting defects in nickel-based single crystal superalloys. Acta Metallurgica Sinica, 2015, 51(10): 1163–1178 (in Chinese)
27. Xuan W, Ren Z, Li C. Experimental evidence of the effect of a high magnetic field on the stray grains formation in cross-section change region for Ni-based superalloy during directional solidification. Metallurgical and Materials Transactions. A, Physical Metallurgy and Materials Science, 2015, 46(4): 1461–1466
28. Ma D, Wu Q, Bührig-Polaczek A. Undercoolability of superalloys and solidification defects in single crystal components. Advanced Materials Research, 2011, 278: 417–422
29. Ma D, Bührig-Polaczek A. Application of heat-conductor technique to production of SC turbine blade. Metallurgical and Materials Transactions. B, Process Metallurgy and Materials Processing Science, 2009, 40(5): 738–748
30. Ma D. Development of single crystal solidification technology for production of superalloy turbine blades. Acta Metallurgica Sinica, 2015, 51(10): 1179–1190 (in Chinese)
31. Ma D, Bührig-Polaczek A. Avoiding grain defects in single crystal components by application of a heat conductor technique. International Journal of Materials Research, 2009, 100(8): 1145–1151
32. Ma D, Bührig-Polaczek A. Development of heat conductor technique for single crystal components of superalloys. International Journal of Cast Metals Research, 2009, 22(6): 422–429
33. Yu J, Xu Q, Cui K, et al. Numerical simulation of solidification process on single crystal Ni-based superalloy investment castings. Journal of Materials Science and Technology, 2007, 23(1): 47–54
34. Napolitano R E, Schaefer R J. The convergence-fault mechanism for low-angle boundary formation in single-crystal castings. Journal of Materials Science, 2000, 35(7): 1641–1659
35. Ma D, Wu Q, Bührig-Polaczek A. Investigation on the asymmetry of thermal condition and grain defect formation in customary directional solidification process. IOP Conference Series: Materials Science and Engineering, 2011, 27: 012037
36. Ma D, Wu Q, Bührig-Polaczek A. Some new observations on freckle formation in directionally solidified superalloy components. Metallurgical and Materials Transactions. B, Process Metallurgy and Materials Processing Science, 2012, 43(2): 344–353
37. Ma D, Bührig-Polaczek A. The influence of surface roughness on freckle formation in directionally solidified superalloy samples. Metallurgical and Materials Transactions. B, Process Metallurgy and Materials Processing Science, 2012, 43(4): 671–677
38. Ma D, Bührig-Polaczek A. The geometry effect of freckle formation in the directionally solidified superalloy CMSX-4. Metallurgical and Materials Transactions. A, Physical Metallurgy and Materials Science, 2014, 45(3): 1435–1444
39. Ma D, Wang F, Wu Q, et al. Innovation of casting techniques for single crystal turbine blades of superalloys. In: Proceedings of International Symposium on Superalloys. 2016, 237–246
40. Ma D, Lu H, Bührig-Polaczek A. Experimental trials of the thin shell casting (TSC) technology for directional solidification. IOP Conference Series: Materials Science and Engineering, 2011, 27: 012036
41. Wang F, Ma D, Zhang J, et al. A high thermal gradient directional solidification method for growing superalloy single crystals. Journal of Materials Processing Technology, 2014, 214(12): 3112–3121
42. Wang F, Ma D, Bogner S, et al. Comparative investigation of the downward and upward directionally solidified single-crystal blades of superalloy CMSX-4. Metallurgical and Materials Transactions. A, Physical Metallurgy and Materials Science, 2016, 47(5): 2376–2386
43. Ma D, Grafe U. Dendrite growth and microsegregation during directional solidification: An analytical model and experimental studies on the superalloys CMSX-4. International Journal of Cast Metals Research, 2000, 13(2): 85–92
44. Ma D, Grafe U. Microsegregation in directionally solidified dendritic-cellular structure of superalloy CMSX-4. Materials Science and Engineering A, 1999, 270(2): 339–342
45. Feng Q, Carroll L J, Pollock T M. Solidification segregation in Ruthenium-containing nickel-base superalloys. Metallurgical and Materials Transactions. A, Physical Metallurgy and Materials Science, 2006, 37(6): 1949–1962
46. Caldwell E C, Fela F J, Fuchs G E. Segregation of elements in high refractory content single crystal nickel based superalloys. In: Proceedings of International Symposium on Superalloys. 2004. 811–818
47. Caldwell E C, Fela F J, Fuchs G E. The segregation of elements in high-refractory-content single-crystal nickel-based superalloys. Journal of Minerals, Metals and Materials, 2004, 56(9): 44–48
48. Heckl A, Rettig R, Singer R F. Solidification characteristics and segregation behavior of nickel-base superalloys in dependence on different rhenium and ruthenium contents. Metallurgical and Materials Transactions. A, Physical Metallurgy and Materials Science, 2010, 41(1): 202–211
49. Wang F, Ma D, Zhang J, et al. Investigation of segregation and density profiles in the mushy zone of CMSX-4 superalloy solidified during downward and upward directional solidification processes. Journal of Alloys and Compounds, 2015, 620: 24–30
50. Wang F, Ma D, Bogner S, et al. Comparative study of the segregation behavior and crystallographic orientation in a nickel-based single-crystal superalloy. Journal of Alloys and Compounds, 2015, 647: 528–532